ARTICLE

Theoretical Investigations on Graphite Oxide Immersed in Water or Methanol

Wan-wan Geng, Wen-hui Zhao, Lan-feng Yuan*

Hefei National Laboratory for Physical Sciences at the Microscale, University of Science and Technology of China, Hefei 230026, China

(Dated: Received on May 28, 2013; Accepted on June 3, 2013)

Different structures of graphite oxide (GO) with and without water are optimized by density functional theory. Without H_2O in interlayer space, the optimized interlayer distances are about 6 Å, smaller than the experimental values of 6.5−7 Å. On the other hand, the interlayer distances of hydrated graphite oxide structures are in good agreement with experimental observations. Based on the optimized GO structures, we then simulate the immersion of GO in water or methanol by molecular dynamics. For the dry GO, water and methanol molecules do not enter the nanopore. While for the hydrated GO, the liquid molecules enter the interlayer space and enlarge the interlayer distance, semi-quantitatively reproducing the experimental phenomena.

Key words: Graphite oxide, Immersion, Density functional theory, Molecular dynamics

I. INTRODUCTION

Although the first preparation of graphite oxide (GO) was as early as in the 1850's by oxidizing graphite with $KClO_3/HNO_3$ [1−4], its structure and chemical composition remains unclear till now, because direct structural information about GO can hardly be obtained. Because of its various interesting properties and close relation with graphene, GO has been used in diverse areas. For example, it is used in thin film technologies because of its hexagonal in-plane structure and ability to be exfoliated layer by layer, and can be used as an insulating material for nanodevices [5, 6]. Large-scale graphene can be produced by GO layers followed by chemical reduction [7, 8]. GO can also be used as a precursor to form polystyrene graphene composites and transparent conducting film [9, 10]. Furthermore, it can be used as the electrodes of batteries and supercapacitors because of its large interlayer distance [11, 12].

Nowadays, GO is obtained by strong oxidation of graphite [13−16]. GO with different oxidation levels can be synthesized by several methods [17−22]. According to the results of NMR, XPS, and IR spectroscopy, several structural models have been proposed for GO [23−25]. It is believed that GO has a layered structure with epoxide and hydroxyl groups distributed on hexagonal carbon layers. The structure is strongly disordered, and the GO sheets are buckled. The carboxyl and alkyl groups are located at the edge of GO flake [21]. In comparison with graphite, whose interlayer distance is 3.4 Å, GO has a significantly increased interlayer distance of 6.5 Å to 7 Å [13, 14].

A unique property of GO is its ability to incorporate polar solvents into interlayer space under ambient conditions. For example, when GO is immersed in water under 1 bar, the water molecules can be easily absorbed into GO, increasing the interlayer distance of GO to ∼11 Å [13−16]. With increase of pressure, the interlayer distance goes up continuously, and at a maximum of 1.3−1.5 GPa the lattice expands by about 28%−30%. Above 1.3−1.5 GPa, the interlayer distance quickly goes down with pressure, and reaches ∼9 Å under 2 GPa. The explanation to this sharp downturn is that in this pressure range the bulk water becomes solid, while water in the interlayer space is still fluid, so no bulk water can be pressed into the nanopore, but interlayer water can be pressed out from the nanopore. This process is reversible, resulting in a unique breathing of the structure upon pressure variation [26]. On the other hand, a high-pressure study of GO immersed in methanol showed a different pattern of interlayer distance *vs.* pressure. Under pressure of 1 bar, the interlayer distance is ∼9 Å, indicating that some methanol molecules enter the GO. But the change in interlayer distance is very small for pressure from 1 bar to 0.2 GPa, so the amount of methanol in the interlayer space should be roughly constant. When the pressure is increased to 0.2−0.8 GPa, a sharp increase of cell volume shows up, reflecting further insertion of methanol into the nanopores. With further increase of pressure, the interlayer distance gradually goes down from the maximum value of ∼12 Å under 0.8 GPa. However, this decrease with methanol is much slower

*Author to whom correspondence should be addressed. E-mail: yuanlf@ustc.edu.cn

than that with water. For example, the interlayer distance of GO/methanol is 11.5 Å under 2 GPa. Therefore, it is inferred that the interlayer methanol molecules are fixed, and cannot be pressed out like the interlayer water molecules [27].

In this work, we study the immersion of GO in H_2O or MeOH at the atomic level, and compare with the experimental results. To obtain a reasonable structure of GO, we first build several models of GO and optimize them with density functional theory (DFT). It is revealed that to get the interlayer distance consistent with its experimental value, the GO model must incorporate H_2O. Based on the optimized GO structures, we then perform molecular dynamics (MD) simulations for GO immersed in water or methanol. It is found that both liquid molecules can enter the nanopore of hydrated GO, consistent with the experimental results.

II. COMPUTATIONAL METHODS AND SIMULATION DETAILS

To incorporate a series of levels of oxidation, we consider three chemical formulae of graphite oxide, *i.e.*, $C_8O(OH)$, $C_8O_2(OH)_2$, and $C_8O(OH)_4$. An issue is that real samples of GO are believed to be hygroscopic in general, and the concentration of water is about 6%−11% in weight [19, 20]. Therefore, we also build models of hydrated GO by introducing one water molecule per chemical formula into the unit cells. This corresponds to H_2O of 14% for the less oxidized GO ($C_8O(OH)$), and 11% and 10% for the two highly oxidized GOs ($C_8O_2(OH)_2$ and $C_8O(OH)_4$), respectively [28]. In the geometry optimizations, several positions are considered for the water molecules.

The density functional calculations are carried out with the Vienna *ab initio* Simulation Package (VASP) [29, 30]. The projector-augmented wave (PAW) method [31, 32] with PBE functional is used for electron-ion interaction, and the Perdew-Wang form [33] of the generalized gradient approximation (GGA) is adopted to describe electronic exchange and correlation. A kinetic-energy cutoff of 500 eV is selected for the plane wave basis set. The Brillouin zone is sampled with a 6×7×2 irreducible Monkhorst-Pack k-point grid [34]. The convergence criteria for force and energy are 0.01 eV/Å and 0.1 meV, respectively.

We then carry out molecular dynamics simulations of GO immersed in H_2O or MeOH using the GROMACS 4.5 software [35]. We pick a 5×5×1 supercell of GO in the optimized geometry, and then put it into a 50 Å×50 Å×50 Å box filled with H_2O or MeOH molecules. NPT simulations are first performed at 300 K and 1 bar, and then the pressure is increased gradually with increment of 0.1 GPa.

The potentials for H_2O and CH_3OH molecules are TIP3P [36, 37] and OPLS united-atom [38, 39] force fields, respectively. The OPLS force field is employed for the GO system, too. The OPLS united-atom methanol model proposed by Jorgensen *et al.* and Haughney *et al.* have been widely used in liquid simulations [40].

TABLE I Structural parameters in optimized configurations of GO structures.

	a/Å	b/Å	c/Å	α/(°)	β/(°)	γ/(°)
$C_8O(OH)$	4.975	4.313	10.763	77.260	89.686	89.979
$C_8O_2(OH)_2$(a)	5.073	4.375	11.539	93.413	82.180	90.004
$C_8O_2(OH)_2$(b)	5.063	4.366	11.952	89.043	101.534	89.914
$C_8O(OH)_4$	5.082	4.408	12.135	86.066	92.122	89.674

III. RESULTS AND DISCUSSION

A. Low oxidation GO: $C_8O(OH)$

Figure 1 shows the optimized configuration of $C_8O(OH)$. Because of the epoxide and hydroxyl groups distributed on hexagonal carbon layers, the GO sheets are puckered. The corresponding cell parameters are listed in Table I. The cell parameters for a sheet are a=4.975 Å and b=4.313 Å, roughly twice of those of graphite, indicating that the sheet structure of GO is similar to that of graphite. The optimized interlayer distance is $c/2$=5.381 Å, which is smaller than the interlayer distances observed by experiment (6.5−7 Å) at ambient temperature and pressure [19, 20]. The most likely reason for this discrepancy is that the pristine samples of GO usually contain water [15−20]. Structures with intercalated H_2O molecules will be discussed later. The distance between an O atom in an epoxide group and an H atom in a OH group of a neighboring layer is 1.945 Å. This length is in the range of hydrogen bonding, and this feature is a determining factor for the interlayer distance.

B. High oxidation graphite oxides: $C_8O_2(OH)_2$ and $C_8O(OH)_4$

We next consider another chemical formula of GO with higher oxygen content, $C_8O_2(OH)_2$, which was also studied in Ref.[19]. Figure 2 (A) and (B) show two local minima configurations of $C_8O_2(OH)_2$. The corresponding cell parameters are listed in Table I, too. The interlayer distance is expanded to 5.770 and 5.976 Å, respectively. As Fig.2(A) shows, the distance between a H atom of an OH group and a neighboring O atom in the same layer is 1.945 Å, shorter than the interlayer hydrogen bonding distance of 2.412 Å. The correponding distance in Fig.2(B) is 2.226 Å, also shorter than the interlayer hydrogen bonding distance of 2.398 Å. Therefore, the intralayer hydrogen bonding is stronger than the interlayer hydrogen bonding.

DOI:10.1063/1674-0068/27/01/9-14

TABLE II Structural parameters in optimized configurations of hydrated GO structures.

	a/Å	b/Å	c/Å	α/(°)	β/(°)	γ/(°)
$C_8O(OH)\cdot H_2O$	4.979	4.315	14.172	89.840	86.397	89.984
$C_8O_2(OH)_2\cdot H_2O$(a)	5.075	4.376	13.676	86.486	84.350	90.042
$C_8O_2(OH)_2\cdot H_2O$(b)	5.069	4.378	14.837	92.676	85.040	89.870
$C_8O(OH)_4\cdot H_2O$	5.083	4.415	15.241	93.908	88.226	89.869

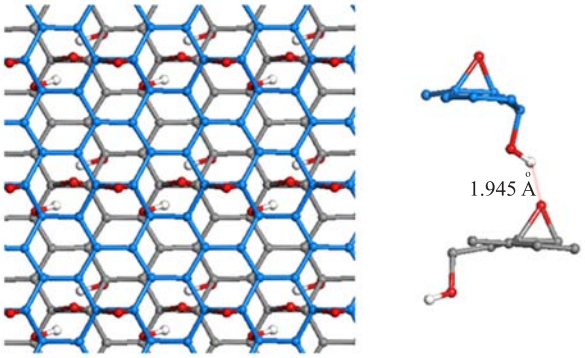

FIG. 1 Optimized configurations of $C_8O(OH)$: top view (left) and side view (right).

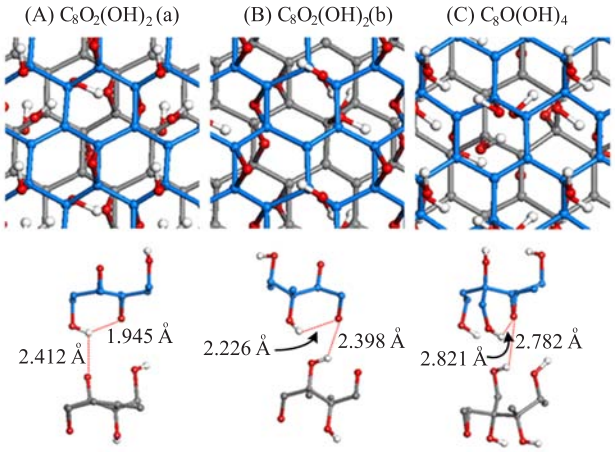

FIG. 2 Optimized configurations of $C_8O_2(OH)_2$ and $C_8O(OH)_4$: top views (up panel) and side views (down panel).

C. Hydrated GO

In general, the pristine sample of GO is not dry, because its preparation usually needs H_2O, and it is hard to separate water from GO. The concentration of water (in weight percentage) is in the range of 6%−11% in real samples [19, 20]. Therefore, it is reasonable to add some number of water molecules into the GO models. So we build the models of $C_8O(OH)\cdot H_2O$ (14%H_2O), $C_8O_2(OH)_2\cdot H_2O$ (11%H_2O), and $C_8O(OH)_4\cdot H_2O$ (10%H_2O). Figures 3 and 4 display the optimized configurations of these compositions, and the corresponding cell parameters are listed in Table II. Their interlayer distances are significantly increased and become close to the range of the experimental values [20]. The origin for this great in-

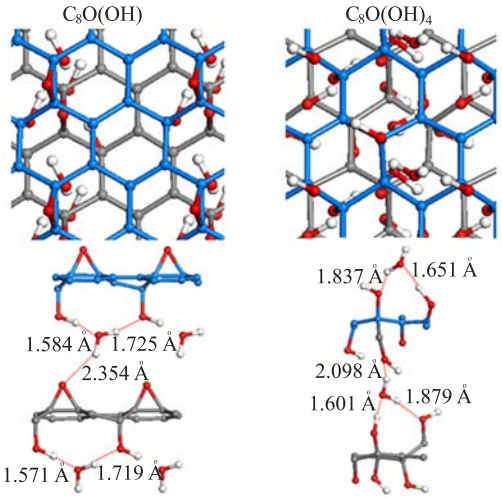

FIG. 3 Optimized configurations of hydrated $C_8O(OH)$ and $C_8O(OH)_4$: top views (up panel) and side views (down panel).

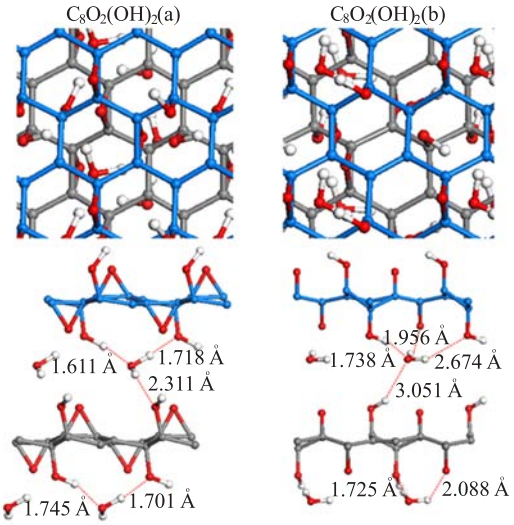

FIG. 4 Optimized configurations of hydrated $C_8O_2(OH)_2$ (a) and (b): top views (up panel) and side views (down panel).

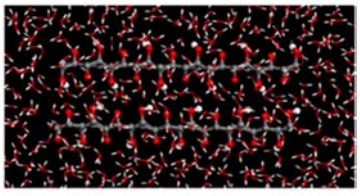

H_2O

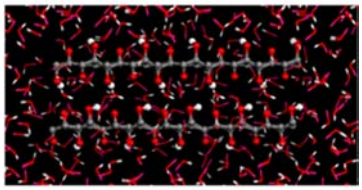

MeOH

FIG. 5 GO immersed in water or methanol at the beginning of molecular dynamics simulations.

crease of interlayer distances lies on the three hydrogen bonds around the H_2O molecule. As for the difference of interlayer distances among different structures, we can also find some tendencies. The higher the degree of oxidation is, the bigger the interlayer distance is. In addition, the distribution of the hydroxyl on different layers also plays a role.

As for the highest oxidation GO species $C_8O(OH)_4$, its configuration is shown in Fig.2(c). The intralayer hydrogen bonding distance is 2.821 Å, close to the interlayer hydrogen bonding distance of 2.782 Å. The interlayer distance is further expanded to 6.068 Å, but still considerably smaller than the experimental values.

D. Molecular dynamics simulations

The GO structures we choose to simulate in an excess of water or methanol are $C_8O_2(OH)_2$(a) and its hydrated counterpart $C_8O_2(OH)_2{\cdot}H_2O$(a), because $C_8O_2(OH)_2{\cdot}H_2O$(a) is the only structure whose interlayer distance (6.84 Å) is in the experimental range of 6.5−7.0 Å, although those of the other hydrated GOs are not far from this range also. Besides, its concentration of H_2O is 11%, in the experimental range of 6%−11%. As a comparasion, the water concentration in $C_8O(OH){\cdot}H_2O$, 14%, is a bit too high.

As the first step, we use two layers of the dry model $C_8O_2(OH)_2$(a) to simulate graphite oxide immersed in water or methanol solution. The simulation starts from 1 bar, and the pressure is increased gradually in step of 0.1 GPa. Every step lasts 8 ns. As shown in Fig.5, in the initial state of the system, there is no fluid molecule between the two sheets of GO. When the simulation goes by, in the interlayer space there is still no water or methanol molecule. Because of this, the interlayer distance does not increase with the pressure as the experimental results. Obviously, this is due to the short interlayer distance of the model (5.77 Å), too much smaller than the experimental value of 6.5−7 Å [27]. Therefore,

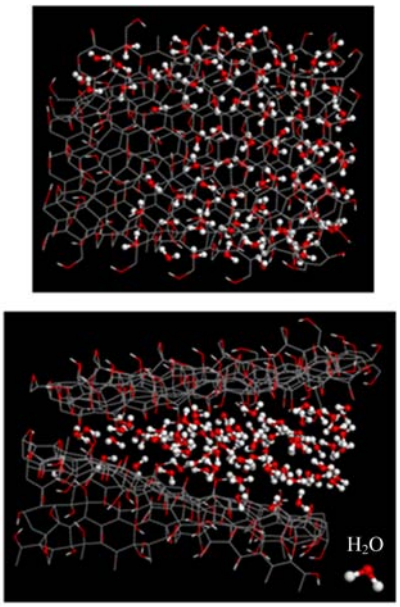

FIG. 6 GO and its interlayer space when immersed in H_2O: top view (up) and side view (down).

the interaction between the layers is too strong, and it is hard for the GO to expand to accommodate solvent molecules.

Then we repeat the simulations for the hydrated model $C_8O_2(OH)_2{\cdot}H_2O$(a). The molecular dynamics simulation starts also from 1 bar, and the pressure is also increased in step of 0.1 GPa, while the time for every step is changed to 20 ns.

As shown in Fig.6 and Fig.7, H_2O or MeOH molecules can now enter into the interlayer space, along with severe distortion of the GO sheets and great increase in the interlayer distance. Therefore, it can be concluded that the initial interlayer distance is crucial when simulating the immersion of GO in liquid. Under the same conditions, the number of water molecules in the interlayer space is more than that of methanol molecules.

Having established the qualitative success of the simulations, we then look at more quantitative details to compare with experiments. When $C_8O_2(OH)_2{\cdot}H_2O$(a) is immersed into water at 300 K and 1 bar, the degree of expansion is similar to the experimental result, namely, a hop from ∼7 Å to ∼11 Å [27]. But with ongoing increase of the pressure, the interlayer distance maintains around 11 Å (Fig.8), in contrast to the experimental behavior of a peak value under 1.3−1.5 GPa [27]. On the other hand, when $C_8O_2(OH)_2{\cdot}H_2O$(a) is immersed into methanol at 300 K and 1 bar, a hop of the interlayer distance is also observed, consistent with experiments, as shown in Fig.9. Nevertheless, the interlayer distance is found to be ∼12 Å, larger than the experimental value of ∼9 Å. Actually, this magnitude is similar to the maximum value in experiments when the pressure is 0.8 GPa [27]. With continuing increase of pressure, the interlayer distance in simulations gradu-

DOI:10.1063/1674-0068/27/01/9-14

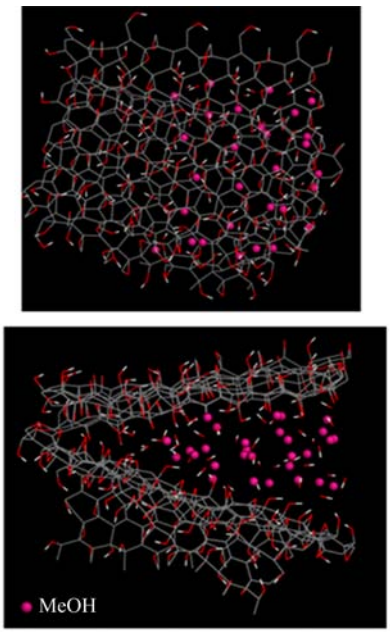

FIG. 7 GO and its interlayer space when immersed in methanol: top view (up) and side view (down).

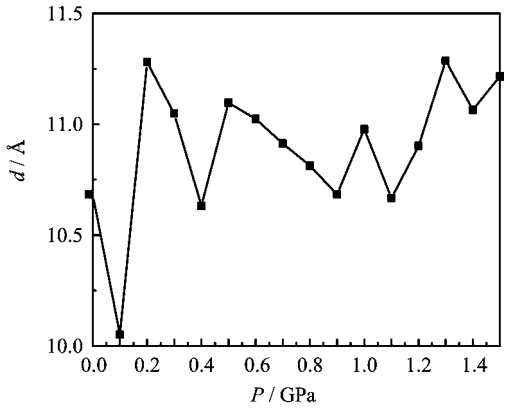

FIG. 8 Interlayer distance d dependence on pressure P of GO/H_2O.

ally decreases, similar to the experimental results above 0.8 GPa.

These discrepancies might be understood from two aspects. Firstly, in experiments, the sudden decrease of interlayer distance under 1.3−1.5 GPa for GO/H_2O is correlated to the solidification of bulk water under this pressure. However, in our additional MD simulation for bulk water with the same force field (TIP3P), it does not freeze under 1.5 GPa, reflecting a drawback of this water model. Therefore, it is no wonder that our simulations for GO/H_2O cannot reproduce this feature. Secondly, we only adopt two layers to mimic a bulk GO, and each layer has only 100 carbon atoms. Given the degree of simplification of our models and their good behaviors on the admissibility of the fluid molecules into the nanopore and on the initial expansion of the interlayer distance, its failure to gain more quantitative results is acceptable.

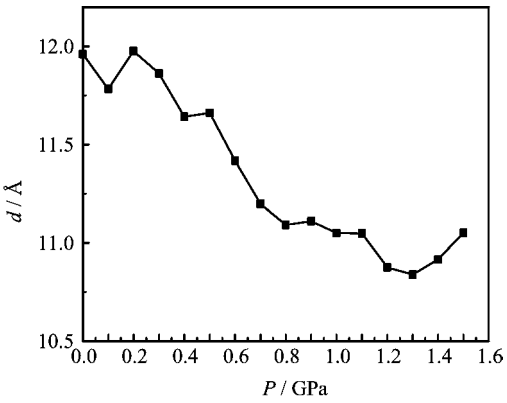

FIG. 9 Interlayer distance d dependence on pressure P of GO/MeOH.

It is interesting to compare the physical pictures of the experiments with our simulations. For GO/H_2O, the simulations agree with the experiments in that the interlayer water is liquid, while the solidification of bulk water under 1.3−1.5 GPa is absent in simulations. For GO/MeOH, the interlayer MeOH molecules cannot be pressed out in both simulations and experiments, but it is too easy for them to enter the nanopore in simulations. To simulate the experimental phenomena with higher precision, we need to build a system with more layers of GO, more carbon atoms per layer, and more solvent molecules.

IV. CONCLUSION

To investigate the immersion of GO in H_2O or MeOH, we optimize GO structures and simulate the immersion processes. Several GO structures with different oxidation levels are considered. To get an interlayer distance close to the experimental value of 6.5−7 Å, it is crucial that the GO structures should contain water. Two layers of the GO structure $C_8O_2(OH)_2$(a) or its hydrated version are tried in MD simulations for immersion. The fluid molecules do not enter the nanopore of the dry GO. On the other hand, both H_2O and MeOH can be inserted into the hydrated GO interlayer space, consistent with experiments. Furthermore, the jumps of the interlayer distance due to this immersion are also evaluated relatively well. We do not get quantitative consistency with experiments on the variation of interlayer distance *vs.* pressure, which is beyond the capability of our highly simplified models. Despite this, these calculations and simulations have deepened our understanding to these fascinating phenomena, and may lead to systematic improvements along this direction.

DOI:10.1063/1674-0068/27/01/9-14

V. ACKNOWLEDGMENTS

This work is supported by the National Natural Science Foundation of China (No.20603032, No.20733004, No.21121003, No.91021004, and No.20933006), the Ministry of Science and Technology of China (No.2011CB921400), the National Excellent Doctoral Dissertation of China (No.200736), the Fundamental Research Funds for the Central Universities (No.WK2340000006, No.WK2060140005, and No.WK2060030012), and the USTC-HP HPC project.

[1] B. C. Brodie, Ann. Chim. Phys. **59**, 466 (1860).
[2] L. Staudenmaier, Ber. Dtsch. Chem. Ges. **31**, 1481 (1898).
[3] B. Brodie, Ann. Chim. Phys. **45**, 351 (1855).
[4] B. C. Brodie, Philos. Trans. R. Soc. London. **A149**, 249 (1859).
[5] R. Ruoff, Nature Nanotechnol. **3**, 10 (2008).
[6] M. Hirata, T. Gotou, S. Horiuchi, M. Fujiwara, and M. Phba, Carbon. **43**, 503 (2005).
[7] V. C. Tung, M. J. Allen, Y. Yang, and R. B. Kaner, Nat. Nanotechnol. **4**, 25 (2009).
[8] S. Stankovich, D. A. Dikin, R. D. Piner, K. A. Kohlhass, A. Kleinhammes, Y. Jia, Y. Wu, S. B. T. Nguyen, and R. S. Ruoff, Carbon **45**, 1558 (2007).
[9] S. Stankovich, D. A. Dikin, G. H. B. Dommett, K. M. Kohlhass, E. J. Zimney, E. A. Stach, R. D. Piner, S. B. T. Nguyen, and R. S. Ruoff, Nature **442**, 282 (2006).
[10] H. J. Shin, K. K. Kim, S. M. Yoon, A. Benayad, H. K. Park, M. H. Jin, H. K. Jeong, J. Kim, J. Y. Choi, and Y. H. Lee, Adv. Funct. Mater. **19**, 1987 (2009).
[11] D. A. Dikin, S. Stankovich, E. J. Zimney, R. D. Piner, G. H. B. Dommett, G. Evmenenko, S. B. T. Nguyen, and R. S. Ruoff, Nature **448**, 457 (2007).
[12] I. J. Kim, S. Yang, M. J. Jeon, S. I. Moon, H. S. Kim, Y. P. Lee, K. H. An, and Y. H. Lee, J. Power Sources **173**, 621 (2007).
[13] W. Scholz and H. P. Boehm, Z. Anorg. Allg. Chem. **369**, 327 (1969).
[14] A. Lerf, A. Buchsteiner, J. Pieper, S. Schöttl, I. Dékány, T. Szábo, and H. P. Boehm, J. Phys. Chem. Solids **67**, 1106 (2006).
[15] A. Lerf, H. He, M. Förster, and J. Klinowski, J. Phys. Chem. B **102**, 4477 (1998).
[16] U. Hofmann and A. Frenzel, Ber. Dtsch. Chem. Ges. **63**, 1248 (1930).
[17] T. Nakajima and Y. Matsuo, Carbon **26**, 357 (1988).
[18] M. Mermoux, Y. Chabre, and A. Rousseau, Carbon **29**, 469 (1991).
[19] T. Szábo, O. Berkesi, P. Forgó, K. Josepovits, Y. Sanakis, D. Petridis, and I. Dékány, Chem. Mater. **18**, 2740 (2006).
[20] H. K. Jeong, Y. P. Lee, R. J. Lahaye, M. H. Park, K. H. An, I. J. Kim, C. W. Yang, C. Y. Park, R. S. Ruoff, and Y. H. Lee, J. Am. Chem. Soc. **130**, 1362 (2008).
[21] H. K. Jeong, H. J. Noh, J. Y. Kim, M. H. Jin, C. Y. Park, and Y. H. Lee, Europhys. Lett. **82**, 67004 (2008).
[22] H. He, J. Klinowski, M. Forster, and A. Lerf, Chem. Phys. Lett. **287**, 53 (1998).
[23] C. Hontoria-Lucas, A. J. López-Peinado, J. D. López-González, M. L. Rojas-Cervantes, and R. M. Martín-Aranda, Carbon **33**, 1585 (1995).
[24] H. He, T. Riedl, A. Lerf, and J. Klinowski, J. Phys. Chem. **100**, 19954 (1996).
[25] A. Lerf, H. He, T. Riedl, M. Forster, and J. Klinowski, Solid State Ionics **101**, 857 (1997).
[26] A. V. Talyzin, V. L. Solozhenko, O. O. Kurakevych, T. Szábo, I. Dékány, A. Kurnosov, and V. Dmitriev, Angew. Chem. Int. Ed. **47**, 8268 (2008).
[27] A. V. Talyzin, B. Sundqvist, T. Szábo, I. Dékány, and V. Dmitriev, J. Am. Chem. Soc. **131**, 18445 (2009).
[28] D. L. Duong, G. Kim, H. K. Jeong, and Y. H. Lee, Phys. Chem. Chem. Phys. **12**, 1595 (2010).
[29] G. Kresse and J. Furthmuller, Comput. Mater. Sci. **6**, 15 (1996).
[30] G. Kresse and J. Furthmuller, Phys. Rev. B **54**, 11169 (1996).
[31] P. E. Blochl, Phys. Rev. B **50**, 17953 (1994).
[32] G. Kresse and D. Joubert, Phys. Rev. B **59**, 1758 (1999).
[33] J. P. Perdew, J. A. Chevary, S. H. Vosko, K. A. Jackson, M. R. Pederson, D. J. Singh, and C. Fiolhais, Phys. Rev. B **46**, 6671 (1992).
[34] H. Monkhorst and J. D. Pack, Phys. Rev. B **13**, 5188 (1976).
[35] B. Hess, C. Kutzner, D. van der Spoel, and E. Lindahl, J. Chem. Theory Comput. **4**, 435 (2008).
[36] W. L. Jorgensen, J. Chandrasekhar, and J. D. Madura, J. Chem. Phys. **79**, 926 (1983).
[37] P. Mark and L. Nilsson, J. Comput. Chem. **23**, 1211 (2002).
[38] M. Haughney, M. Ferrario, and I. R. McDonald, Mol. Phys. **58**, 849 (1986).
[39] W. L. Jorgensen, J. Chandrasekhar, J. D. Madura, R. W. Impey, and M. L. Klein, J. Chem. Phys. **79**, 926 (1983).
[40] C. J. Shih, S. C. Lin, R. Sharma, M. S. Strano, and D. Blankschtein, Langmuir **28**, 235 (2012).

DOI:10.1063/1674-0068/27/01/9-14